Thin-Walled Structures 138 (2019) 243–251

Contents lists available at ScienceDirect

Thin-Walled Structures

journal homepage: www.elsevier.com/locate/tws

Full length article

Experimental study on fatigue performance of Q460 and Q690 steel bolted connections

Hongchao Guo[a,b,*], Kuanhong Mao[a,b], Yunhe Liu[a,c], Gang Liang[b]

[a] State Key Laboratory Base of Eco-hydraulic Engineering in Arid Area, Xi'an University of Technology, No.5 Jinhua Road, Xi'an 710048, PR China
[b] School of Civil Engineering and Architecture, Xi'an University of Technology, No.5 Jinhua Road, Xi'an 710048, PR China
[c] Institute of Water Resources and Hydro-electric Engineering, Xi'an University of Technology, No.5 Jinhua Road, Xi'an 710048, PR China

ARTICLE INFO

Keywords:
High-strength steel
Bolted connection
Fatigue limit
Fatigue performance
Stress concentration

ABSTRACT

In this paper, we present an experimental study of the fatigue performance of high-strength steels base materials, perforated plate, and bolted connection. The corresponding fatigue life was predicted. According to the stress concentration degree, the location of the initial crack was discussed, and the reduction degree in fatigue strength was quantitatively analyzed by the fatigue notch factor. Finally, the fatigue damage development process was analyzed on the basis of fatigue damage theory. Results indicated that the base materials and perforated plate showed good fatigue performance in the finite fatigue range. Their fatigue limit was clearly higher than the code value. The fatigue strengths of the Q690 base material and the perforated plate under the 95% survival probability were 1.3 and 1.2 times that of Q460, respectively. The fatigue performance of bolted connection Q690 was significantly higher than of Q460. Under the 95% survival probability, the fatigue strength of bolted connection Q690 was 1.5 times that of Q460. The stress concentration led to enhanced local stress and stress gradient. It also restricted crack initiation at maximum stress and reduced the fatigue strength of specimens. Damage value could better reflect the internal state changes of the components well in the process of fatigue failure. With the fatigue cycles times increased , the damage value gradually increased, whereas the effective bearing area and bearing capacity decreased, and the instantaneous fracture occurred.

1. Introduction

Bolted connections are used as an efficient and versatile joining technology in a variety of engineering applications. It is seen as a good alternative to welded equivalents. Bolted connections are rather simple to assemble even in challenging conditions and have the advantage that they can be disassembled and reassembled numerous times. However, the stress concentration in the opening area of the plate in the bolt connection is severe, and brittle fracture is prone to occur under the alternating load. Fatigue damage has no obvious plastic deformation, and sudden damage often leads to catastrophic accidents, causing huge economic losses.

Results of related research indicated that the fatigue strength of bolted connections is affected by various factors, such as bolt pretension force, bolt arrangement, friction surface treatment, steel grade, and opening ratio [1]. Sehitoglu [2] predicted the fatigue life of open-hole specimens based on local strain and elastoplastic fracture mechanics theory. Josi et al. [3]. studied the fatigue performance of double-lap staggered holes. In the calculation of fatigue life, considering the influence of average stress, Morrow [4] and SWT [4] models were proposed based on stress and strain methods. Both models are well prediction for fatigue life. Alegre and Sanchez [5,6] showed that the fatigue strength of drilled hole components is twice that of punched hole components according to the fatigue test results of perforated plates. Minguez [7] investigated the effects of the bolt pretension force on fatigue life of an aluminum alloy bolted connection , The results show that in the single lap joint connection, the fatigue life does not change significantly with the increase of the pretension force. The greater pretension force of double-lap bolted connection, the fatigue life gets longer correspondingly. Benhamena [8,9] research shows that when the pretension force of the bolt is low, the crack appears where is easy to generate stress concentration in the bolt hole. Increasing the pretension force of the bolt can alleviate the stress concentration, and the cracking position is transferred to the front of the hole,and the fatigue life is increased. Saranik [10] studied the low cycle fatigue performance of bolted joints. The bolts were loosened under repeated

* Corresponding author at: School of Civil Engineering and Architecture, Xi'an University of Technology, No.5 Jinhua Road, Xi'an City, Shaanxi Province 710048, PR China.
E-mail address: ghc-1209@163.com (H. Guo).

https://doi.org/10.1016/j.tws.2019.02.011
Received 28 April 2018; Received in revised form 5 January 2019; Accepted 13 February 2019
Available online 20 February 2019
0263-8231/

Table 1
Specimens category.

Steel grade	Group type	Specimen type	Number	Steel grade	Group type	Specimen type	Number
Q460D	A	Base metal	15	Q690D	D	Base metal	13
	B	Perforated plate	15		E	Perforated plate	13
	C	Bolted connection	15		F	Bolted connection	13

excitation, the micro-sliding between the joint plates, the stress redistribution, and the fatigue damage gradually occurred. Wang [11,12] studied the hole forming method of bolted joints and the influence of bolt pretension force on the fatigue life of the components. Janne et al. [13] study different operating and design parameters of a single bolted joint on the fretting fatigue life. The results show that fretting significantly decreases fatigue life in bolted joints. These studies have focused on the fatigue performance of normal steel bolted connection.

Recent years, with the improvement of steel production technology and the maturity of corresponding welding materials and joining technologies, high strength steel has been successfully applied in many buildings. High strength steel improves the strength, plasticity and fracture toughness of steel thanks to specific Thermo-Mechanical Control Process (TMCP) and the addition of alloying elements, and has good fatigue properties. At present, in the study of fatigue properties of high strength steel, Chen et al. [14] studied the fatigue properties of high-strength steel based on stress, strain and energy methods. Studies have shown that high strength steel exhibit slightly higher fatigue resistance than normal steels. Davies [15] research shows that high-strength steel has high hardness and is sensitive to stress concentration, which has a significant effect on structural fatigue life. Jezernik [16] believes that the surface roughness of high strength steel has a significant effect on fatigue strength. Cicero et al. [17,18] investigated the effects of oxy-fuel, plasma, and laser cutting techniques on the fatigue performance of high strength steel and provided the corresponding BS7608 code design grades. Only in the aerospace and mechanical fields, Carlos et al. [19] studied the fatigue failure mechanism of high strength steel bolt joints under different pretension force levels. The experimental results reveal that an increase in the pretension force significantly improves the fatigue life of the bolt connection. Hämäläinen [20] has reported the susceptibility to fretting fatigue of bolted connections made of S960QC and the possible challenges linked to it. It is noteworthy that design rules for bolted connections are widely available in European standards [21,22] together with extensions to include higher steel grades [23]. The fatigue strength curves and detail categories in [24] are mainly based on fatigue tests carried out on bolted and welded carbon steels details with nominal yield stress ranging from 235 to 400 MPa. And, even if the part 1–9 may cover higher structural steel grades given in EN 1993-1-12 (S235-S700), the phenomena governing the fatigue resistance of HSS bolted joints are currently not perfectly known.

Fatigue damage to civil structures doesn't endanger life as much as aerospace structures. The ultimate goal of fatigue analysis is to determine the fatigue life of structures or components, and to provide classification of connections and allowable stress amplitude according to detail construction, which provides standards and basis for structural design. There are relatively few studies on the fatigue properties of high strength steel under different joint structures. In this paper, high strength steel base material was used as the comparative specimen, and the fatigue performance test of Q460 and Q690 high strength steel perforated plate and bolt connection was carried out. The S-N curve was fitted and the fatigue characteristics and fatigue life of the base material, perforated plate and bolted joints was evaluated using BS7608 [25], Eurocode3 [26] and AISC360 [27]. Through the comparison of the fatigue strength of the base material, perforated plate and bolt connection, the influence of stress concentration and standard pretension force on fatigue strength is analyzed. The crack initiation position was analyzed from the macroscopic level. And the damage curve is used to analyze the development process of fatigue damage.

2. Testing arrangement and specimen details

2.1. Specimen design

In order to study the fatigue characteristics and laws of high strength steel bolted connection, referring to GB/T 2975-1998 "Steel and Steel Products-Location and Preparation of Test Pieces for Mechanical Testing" [28], the test materials using 8 mm thick Q460D and Q690D high strength steel and it is sampled at full thickness. Three group specimens were designed for this test material. The specimens were divided into base material, perforated plate and bolted connection. The detailed classification is shown in Table 1. The geometric dimensions of the specimens are shown in Fig. 1. The aperture of the perforated plate specimens was 22 mm. The bolted connection specimens were double-shear joints, and the aperture was 22 mm. The bolt–hole edge distance, end distance, and bolt pitch satisfied the GB50017-2018 [29] connection construction requirement. Grade 10.9 M20 high-strength bolts were used to assemble the main plate and the connecting plate. The perforated plate specimens bore 510 N·m torque to achieve the specified pretension. Table 2 lists the chemical compositions of the steel materials.

2.2. Material properties

The test materials were High-strength low-alloy rolling steels fabricated in ShouGang, a famous steel company in China. Their material parameters were tested according to the "Tensile Test of Metal Materials Part I: Experimental Method under Room Temperature" (GB/T 228.1-2010) [30]. The stress-strain curves of the high strength steel were plotted (Fig. 2). Table 3 lists the corresponding mechanical properties. Static tensile tests were performed on the base material, perforated plate, and bolted connection, and its corresponding yield loads were obtained (Table 4). The yield load values of the specimens were determined by a fatigue test.

2.3. Test setup and loading procedure

This fatigue loading experiment was accomplished on an MTS322 electrohydraulic servo fatigue tester. The loading waveform was a constant amplitude sinusoid. PVC compensation was used, and the stress ratio in cyclic loading was set as $R = S_{min}/S_{max} = 0.1$. The loading frequency fluctuated at a range of 15–30 Hz. The maximum stress level of the fatigue test was determined by the yield strength of specimens. Specimens were maintained at an elastic state throughout the experiment. The initial maximum stress (S_{max}) was determined to be 0.6 f_y to 0.8 f_y. The fatigue limit was determined according to the small sample up-and down method and gradually approached by adjusting the loading coefficient. i.e., the stress level of the specimen which was broken by repeated load at 2 million times. The experiment was ended upon the presence of anomalies and fractures or upon reaching 2 million cycles number.

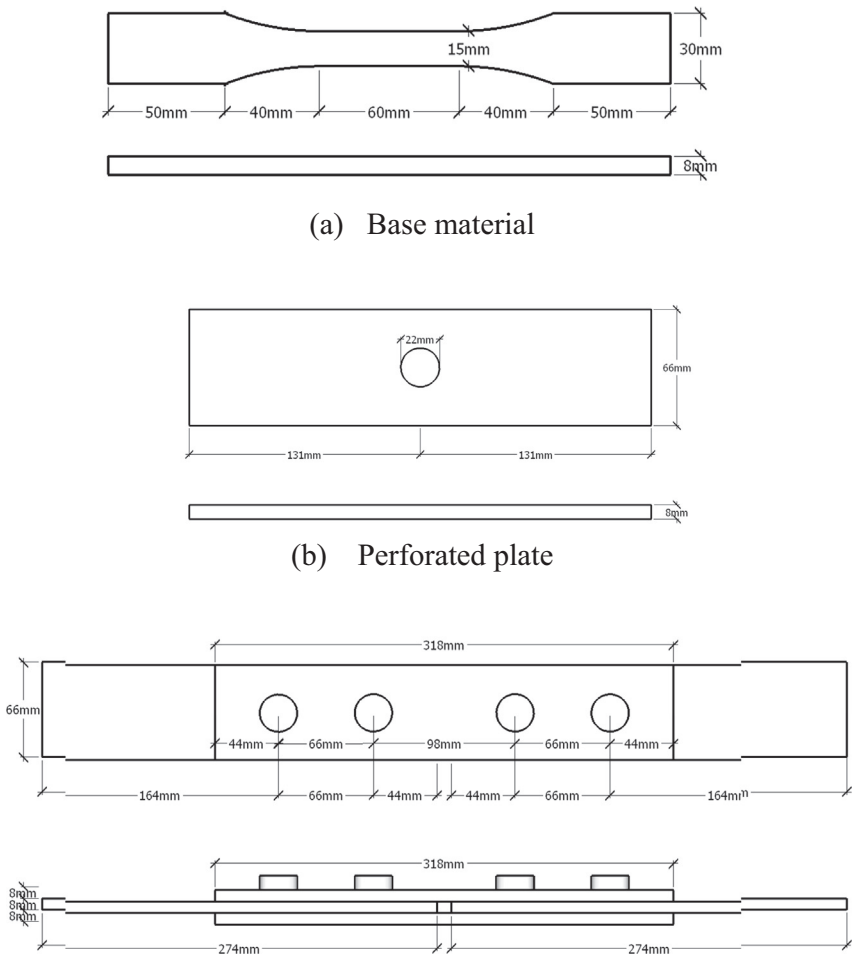

Fig. 1. The geometry size of specimen.

Table 2
Chemical compositions of steel and electrode (%).

Chemical compositions	C	Mn	Si	P	S	Ni	Cr	Mo	V
Q460D	0.08	1.09	0.15	0.011	0.002	0.50	0.55	0.08	0.075
Q690D	0.07	1.6	0.15	0.008	0.001	–	0.01	0.002	0.002

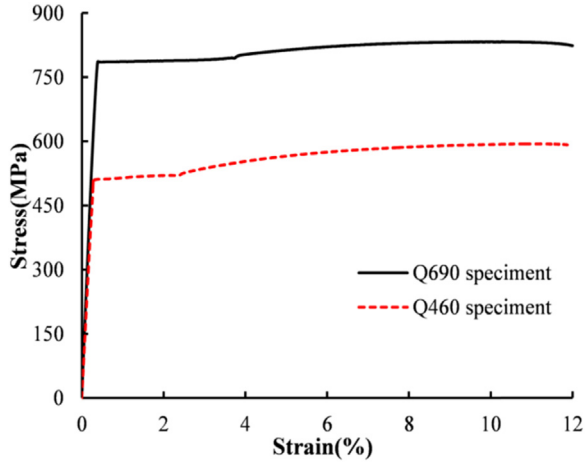

Fig. 2. Stress-strain curves.

Table 3
Material characteristic test result.

Steel grade	Tensile strength (Mpa)	Yield strength (Mpa)	Elastic modulus (×105 MPa)
Q460D	592.0	504.9	2.524
Q690D	832.0	786.3	2.063

Table 4
Yield load value of specimen.

Specimen type	Base metal	Perforated plate	Bolted connection
Q460 yield load (kN)	60.59	180.00	189.52
Q690 yield load (kN)	94.36	220.45	281.51

3. Theoretical analysis

The relationship between external loads and fatigue life should be established to estimate the fatigue life or fatigue strength. The relationship curve between reaction loads and fatigue life is called the *S–N* curve. The empirical equation of the *S–N* curve in the form of a power function is expressed as follows:

$$S^m N = C, \tag{1}$$

where S is the nominal stress amplitude of the specimen section and C and m are fatigue parameters related to a component type.

In the *S–N* curve, generally, the abscissa axis of the logarithm denotes the cycle number and the vertical axis of the logarithm denotes the stress amplitude or maximum stress. By calculating the logarithm of the two sides of Eq. (1), we can obtain the following expression:

$$\lg N = \lg C - m \lg S. \tag{2}$$

3.1. BS7608

BS7608 [25] is based on linear damage accumulation theory. BS7608 divides the connection joint into B, C, D, E, F, F2, G, G2, W1, X, S1, S2, and TJ13 levels according to the local stress concentration, loading direction, possible crack initiation position, and geometric shape of the joint. This standard summarizes abundant fatigue test data, provides fatigue calculation methods for different connection forms, and effectively supports the fatigue life prediction of different connection structures.

For different design levels, the relationship between stress amplitude (S) and the number of fatigue failures (N) is as follows:

$$\lg N = \lg C_0 - d\sigma - m \lg S, \tag{3}$$

where $\lg C_0$ is related to the mean *S–N* curve, σ is the standard deviation of the corresponding design level, m is the slope of the *S–N* curve under the log–log coordinates, and d is the coefficient related to the test level.

Using Formula (3), we derive the following equation:

$$\lg C = \lg C_0 - d\sigma, \tag{4}$$

Eq. (4) can be rewritten as following:

$$S^m N = C \quad . \tag{5}$$

3.2. Eurocode3

Eurocode3 (EC3) [26] uses a limit state design method that is based on probability theory and is applied for the fatigue design of steel structures as a partial factor. The fatigue fracture of steel structures belongs to the ultimate limit state. Previous research has shown that stress amplitude is one of the main factors that influences the fatigue strength of structures. Base on the stress amplitude and fatigue strength, the fatigue failure expression under the ultimate stress state can be set as follows:

$$\Delta\sigma_R - \Delta\sigma_S = 0, \tag{6}$$

where $\Delta\sigma_R$ is the fatigue strength determined by the structural detail classification *S–N* curve and $\Delta\sigma_S$ is the equivalent stress amplitude caused by fatigue load. The fatigue strength curve is also called the *S–N* curve, which can be obtained through the regression analysis of fatigue test data. The logarithmic linear equation is expressed as follows:

$$\lg N = \lg C - m \lg \Delta\sigma, \tag{7}$$

where $\Delta\sigma$ is the stress amplitude and C and m are the performance parameters of the structures or materials.

The fatigue life discreteness was large under the same stress level due to changes in material properties, processing conditions, fatigue loading, test process, and the fatigue fracture of specimens. Fourteen fatigue strength curves of normal stress amplitude and two fatigue strength curves of shear stress amplitude were provided in Eurocode3.

The fatigue strength design curves of the normal stress amplitude when $N \le 5 \times 10^6$ were expressed as the following:

$$\Delta\sigma_R^m N = \Delta\sigma_C^m 2 \times 10^6, \tag{8}$$

where $m = 3$ and $\Delta\sigma_C$ is the stress amplitude corresponding to the 14 fatigue strength design curves of the normal stress amplitude in EC3 when $N = 2 \times 10^6$.

When $5 \times 10^6 \le N \le 10^8$, the following formula is used:

$$\Delta\sigma_R^m N = \Delta\sigma_C^m 5 \times 10^6, \tag{9}$$

where $m = 5$ and $\Delta\sigma_C$ is the stress amplitude corresponding to the 14 fatigue strength design curves of the normal stress amplitude in EC3 when $N = 10^8$.

3.3. ANSI/AISC360-10

ANSI/AISC360-10 [27] defines the ultimate limit state from fatigue cracking to failure in the range of elastic stress. The stress range of different stress types should not exceed the following regulations:

For stress types A, B, B', C, D, E, and E', the allowable stress amplitude (F_{SR}) is determined using the following equation:

$$F_{SR} = \left(\frac{C_f \times 329}{N}\right)^{0.333} \ge F_{TH}, \tag{10}$$

where C_f is the constant related to stress type and is determined according to fatigue type, F_{SR} is the allowable stress amplitude, and F_{TH} is the threshold allowable stress amplitude.

For stress type F, F_{SR} was determined using the following formula:

$$F_{SR} = \left(\frac{C_f \times 11 \times 10^4}{N}\right)^{0.167} \ge F_{TH} \quad . \tag{11}$$

4. Fatigue results

4.1. Fatigue test results

Fatigue tests were conducted on 84 Q460 and Q690 specimens, which yielded 39 and 32 effective test data, respectively. Tables 5–6 record the results. The fracture position at base material was close to

Table 5
The fatigue test parameter and results of Q460D bolted connections.

Specimen number	K	Smax (MPa)	N (Cycle)	Specimen number	K	Smax (MPa)	N (Cycle)	Specimen number	K-	Smax (MPa)	N (Cycle)
A-1-460	0.80	363.53	439443	B-1-460	0.70	322.16	127248	C-1-460	0.80	387.66	474712
A-2-460	0.78	354.44	431262	B-2-460	0.60	276.14	141135	C-2-460	0.80	387.66	416493
A-3-460	0.76	345.35	1245455	B-3-460	0.55	253.13	432064	C-3-460	0.75	363.43	946656
A-4-460	0.75	340.81	1072197	B-4-460	0.55	253.13	392275	C-4-460	0.75	363.43	990290
A-5-460	0.74	336.26	383206	B-5-460	0.50	230.11	383722	C-5-460	0.70	339.19	730641
A-6-460	0.72	327.18	781228	B-6-460	0.45	207.10	458040	C-6-460	0.65	314.97	1409507
A-7-460	0.70	318.09	476435	B-7-460	0.44	202.50	561951	C-7-460	0.60	290.74	1632635
A-8-460	0.70	318.05	754243	B-8-460	0.43	197.90	848352	C-8-460	0.55	266.52	2000000
A-9-460	0.69	313.54	2000000	B-9-460	0.429	197.44	2000000	C-9-460	0.55	266.52	1077294
A-10-460	0.69	313.54	1258629	B-10-460	0.428	196.88	2000000	C-10-460	0.54	259.88	1039349
A-11-460	0.67	304.45	729495	B-11-460	0.425	195.60	2000000	C-11-460	0.50	242.28	1765546
A-12-460	0.65	295.37	2000000	B-12-460	0.42	193.30	2000000	C-12-460	0.48	232.59	2000000
A-13–460	0.65	295.37	2000000	B-13–460	0.40	184.09	2000000	C-13-460	0.45	218.05	2000000

Where K represents loading coefficient, A series represents base material, and B series represents perforated plate, and C series represents bolted connection.

Table 6
The fatigue test parameter and results of Q690D bolted connections.

Specimen number	K	Smax (MPa)	N (Cycle)	Specimen number	K	Smax (MPa)	N (Cycle)	Specimen number	K	Smax (MPa)	N (Cycle)
D-1-690	0.70	495.40	267166	E-3-690	0.512	288.59	211750	F-2690	0.7	335.90	429155
D-2-690	0.65	460.01	291355	E-4-690	0.48	270.55	261710	F-3-690	0.65	337.47	542759
D-3-690	0.62	438.78	275873	E-5-690	0.45	253.64	561678	F-4-690	0.60	287.91	772436
D-4-690	0.6	424.63	501540	E-6-690	0.44	248.01	702857	F-5-690	0.598	287.10	1201886
D-5-690	0.59	417.55	1822432	E-7-690	0.435	245.19	681557	F-6-690	0.55	263.91	941025
D-6-690	0.58	410.47	2000000	E-8-690	0.435	245.19	2000000	F-7-690	0.53	254.32	1360300
D-7-690	0.57	403.40	2000000	E-9-690	0.43	242.37	2000000	F-8-690	0.524	251.22	1046198
D-8-690	0.56	396.32	2000000	E-10-690	0.42	236.73	2000000	F-9-690	0.51	244.72	1018837
D-9-690	0.55	389.24	2000000	E-11-690	0.41	231.10	2000000	F-10-690	0.50	239.93	2000000
E-1-690	0.70	394.56	111941	E-12-690	0.4	225.46	2000000	F-11-690	0.48	230.32	2000000
E-2-690	0.597	336.89	132258	F-1-90	0.8	383.88	306399				

Where K represents loading coefficient, D series represents base material, and E series represents perforated plate, and F series represents bolted connection.

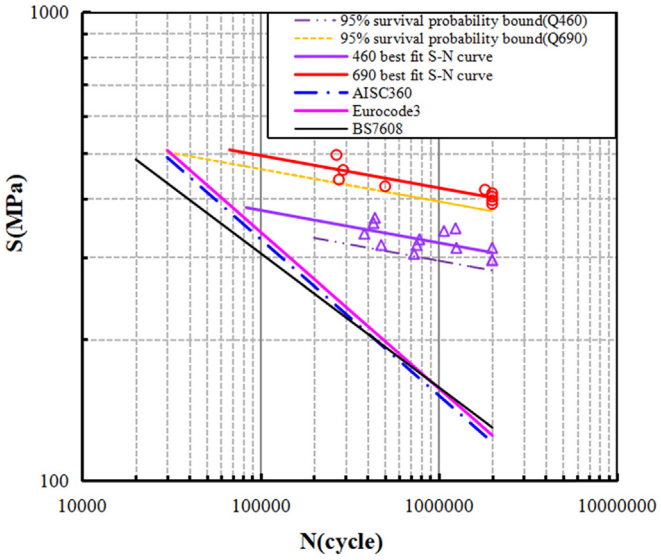

Fig. 3. Fatigue test result for base metal.

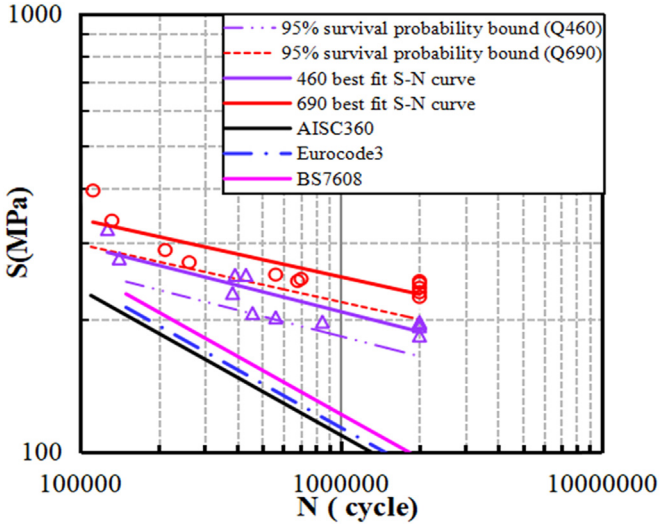

Fig. 4. Fatigue test result for perforated plate.

the arc transition section. The perforated plate was broken at the net cross section and the bolted connection specimens were broken in the area before the first row of holes. Figs. 3–5 illustrate the effective test data. The *S–N* curve was obtained from the regression analysis of the test data.

To evaluate the test data, we illustrated the corresponding European code, American code, and UK code fatigue design curves in the figures. The fatigue limit values of 2 million cycles were determined (Table 7).

The following features were observed in Figs. 3–5.

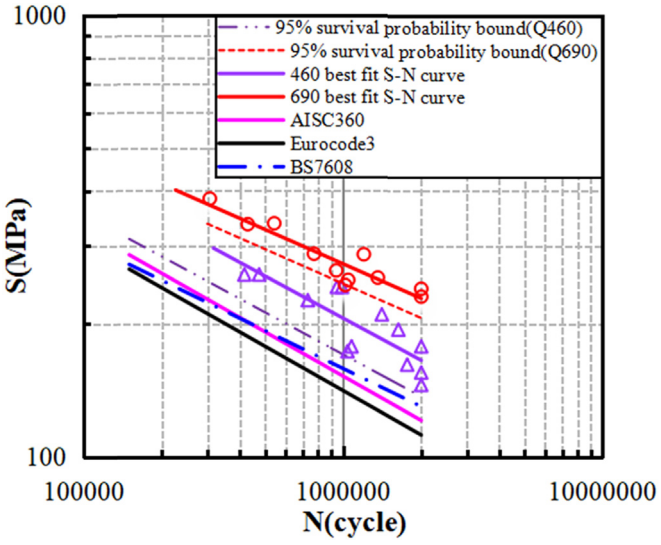

Fig. 5. Fatigue test result for bolted connection.

(1) The test data is more discrete, and the fatigue life is more discrete at the same stress level, but conformed to the trend that the lower the stress level, the longer the fatigue life.
(2) For the base material, the fatigue performance of the AISC360, BS7608, and EC3 design curves exhibited a similar trend. All test data were positioned above the code curves. The base materials of Q460 and Q690 showed good fatigue performance in the finite fatigue range. The fatigue strength was significantly higher than the code value. For fatigue life estimation of the Q460 and Q690 base materials, the code method was relatively conservative. Under the 95% survival probability , the fatigue strength of the Q690 base material was 1.3 times that of the Q460 base material. The fatigue strength was related to the degree of steel strength. As the ultimate strength of steel increases, the fatigue strength increases.
(3) The *m* values of the perforated plate code curve are all 3. The fitting curves of the Q460 and Q690 perforated plates were above the code curves, and the m value was greater than 3. Under the 95% survival probability, the fatigue strengths of the Q690 perforated plate were 2.3times, 2.1times, and 2.2 times of the code values of AISC360, BS7608, and Eurocode3, respectively. For the Q460 perforated plate, its fatigue strengths were 1.9times, 1.7times, and 1.8 times of the code values ofAISC360, BS7608, and Eurocode3, respectively. The perforated plates showed good performance in the finite fatigue range, and the code values were relatively conservative. The fatigue

Table 7
Comparison of fatigue limit values.

Specimen type	Q460 fitted value (MPa)	95% survival probability (MPa)	Q690 fitted value (MPa)	95% survival probability (MPa)	AISC360 value (MPa)	BS7608 value (MPa)	Eurocode3 value (MPa)
Base metal	306.53	280.60	401.70	375.63	120.81	129.88	125
Perforated plate	187.77	165.06	228.78	200.47	86.5	96.61	90
Bolted connection (gross section)	165.26	136.77	228.28	205.96	120.81	129.88	112

strength under the 95% survival probability of Q690 was 1.2 times that of Q460. The fatigue strength of the perforated plates increased with the limit strength of the steel.

(4) For the bolted connections, the AISC360 and EC3 design curves were parallel. The AISC360 and BS7608 design curves were applicable for the fatigue life analysis of the bolted connection of Q460 and showed adequate safety margins. In comparison with the AISC360 curve, the EC3 curve was relatively conservative. In the finite fatigue range, the fatigue performance of the Q690 bolted connection was significantly superior to that of the Q460 bolted connection. The fatigue strength under the 95% survival probability of Q690 was 1.5 times that of Q460, which indicated that the fatigue strength of the bolted joints was related to the limit strength of the steel. The fatigue strength increased with the limit strength of the steel. Therefore, for the fatigue performance evaluation of the Q690 bolted connection, the code method was relatively conservative.

4.2. Analysis of fatigue strength of different structures

Where the geometric shape of the component section changed suddenly , the local stress was greater than the nominal stress , which was called stress concentration. The stress concentration increases the local stress of the notch. In the elastic range, the stress concentration effect generated by the notch can be characterized by the theoretical stress concentration factor K_t [31]. Under the same conditions, the larger the stress concentration factor K_t, the lower the fatigue strength value. However, the stress concentration factor K_t does not reflect the degree of influence of stress concentration on fatigue strength. It is generally characterized by the fatigue notch coefficient K_f. The fatigue notch coefficient K_f is the ratio of the fatigue limit of the smooth sample to the notched specimen under the same materials, dimensions and loading conditions. The fatigue notch coefficient K_f indicate the degree to which the fatigue strength is actually reduced. The calculation formula is as follows:

$$\frac{K_t}{K_f} = 0.88 + AQ^b \tag{12}$$

where Q is the relative stress gradient and A and b are the constants for the heat treatment methods.

The theoretical calculation of the fatigue notch coefficients of the base materials and perforated plates were1.06 and 2.14, respectively. The fatigue notch coefficients of the perforated plates is about 2 times higher than that of the base material. For comparison, Figs. 6–8 shows the fatigue test compare results for the base materials, perforated plates, and bolted connections. Table 8 shows the fatigue strength values for different cycle number under a 95% probability. As can be seen from Fig. 6 and Table 8: when N = 2 million times, calculation by net section, the fatigue strength of the Q460 and Q690 perforated plate with opening ratio of 2.2% was 41.18% and 46.63% lower than corresponding base material, respectively. Calculation by gross section, the fatigue strength of the perforated plate was 56.43% and 60.46% lower than corresponding base material, respectively. The fatigue strength of the Q690 perforated plate was 17.66% higher than that of the Q460. It is shown that the stress concentration has a great effect on the fatigue strength of high strength steel, and it is also verified that the fatigue

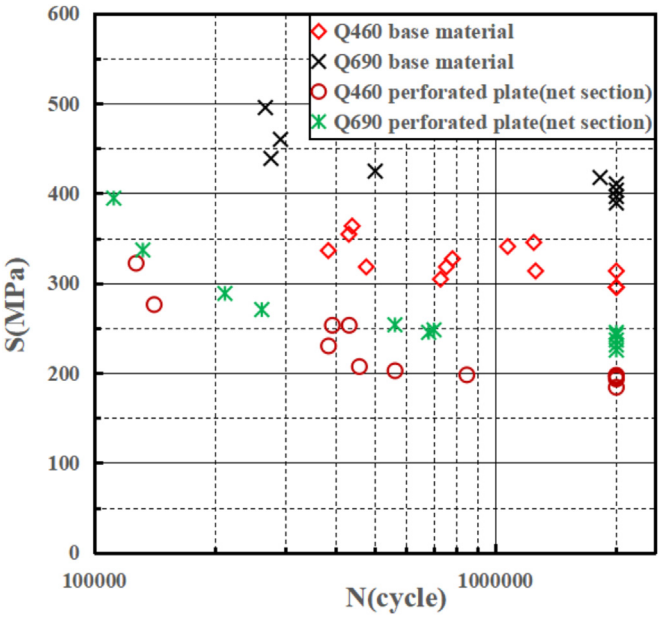

Fig. 6. Comparison of fatigue test results between base material and perforated plate.

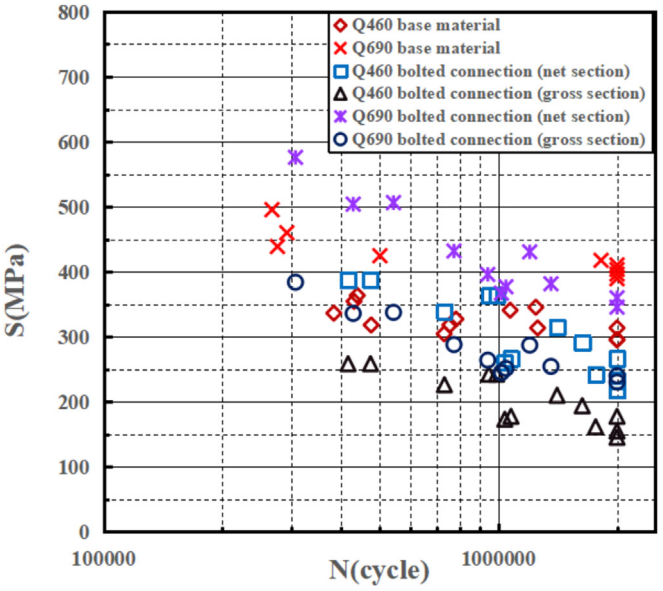

Fig. 7. Comparison of fatigue test results between base material and bolted connection.

strength of the perforated plate increases as the increase of the ultimate strength of the steel. The features were observed in Figs. 7–8 and Table 8, when $N \leq 5 \times 10^5$ times, the fatigue strength of the Q460 and Q690 bolted connection calculated by the net section is slightly higher than that of the corresponding base metal; When N = 2 million times,

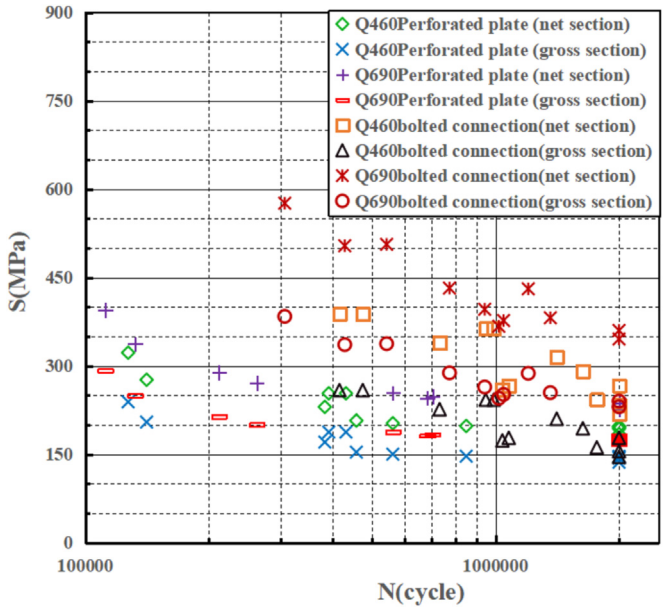

Fig. 8. Comparison of fatigue test results between perforated plate and bolted connection.

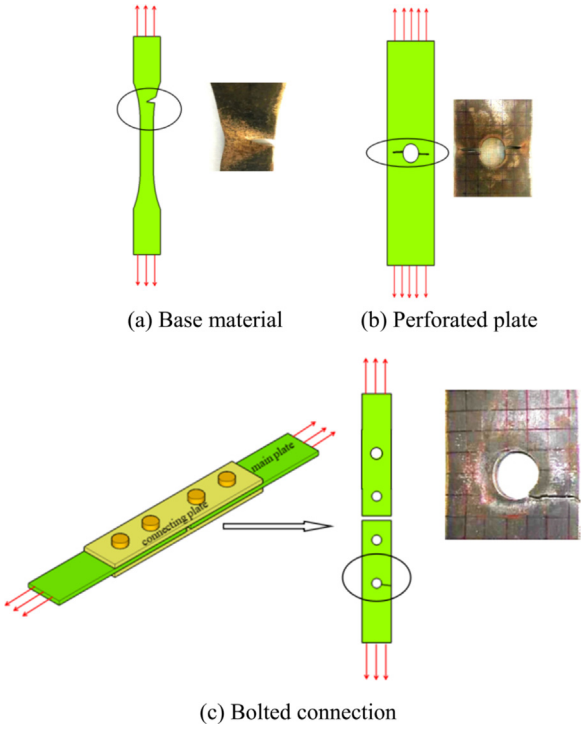

Fig. 9. Failure modes.

the fatigue strength of the Q460 and Q690 bolted connection calculated by the net section is 26.9% and 17.75% lower than that of the base metal; Calculation by net section, the fatigue strength of the Q460 and Q690 bolted connection was 19.53% and 35.11% higher than those base material, respectively. The fatigue strength calculated by the gross section is 10.60% and 27.89% higher than that of the perforated plate, respectively. The fatigue strength of the Q690 bolted connection is 41.18% higher than that of the Q460 bolted connection. It shows that the external force is transmitted through the friction between the main board and the splice plate after applying the standard pretension, the pressure between the plates is increased, this greatly alleviates the stress concentration around the bolt holes, thereby increasing the fatigue strength of the bolt connection. The conclusion that the fatigue strength of the bolted connection increases as the ultimate strength of the base material increases also applies to the high strength steel.

4.3. Fatigue failure mode

Fig. 9 lists the macroscopic failure modes of the fatigue specimens. The base material was a round specimen with a shoulder. Due to the sudden change in the section of the arc transition, stress concentration occurs, so the fracture position is transitioned from the arc to the parallel section The stress concentration of the perforated plate specimen is too large at the opening hole, and the fatigue crack is generated at the net cross section of the hole and extends along the center of the net cross-section hole wall in the direction perpendicular to the load ; The fatigue failure mode of the base materials and perforated plates showed that the fatigue crack easily occurred at the area of stress concentration. For the bolted connections, the steel plates around the bolt hole were compressed and radially expanded because of the bolt pretension force. After the compression was constrained, the compressive stress was generated in the circumferential direction, which weakened the degree of stress concentration by tensile stress at the hole edge , and prevented the fatigue crack from forming at the net section. The fatigue crack transferred to the front area of the hole. Therefore , the bolt connection breaks in the area of the first row of bolt holes, and the fatigue crack gradually develop along the front section of the bolt hole of the main board. The three sets of test pieces did not undergo major deformation before the damage, and all belonged to brittle failure.

The fatigue section of the base material was scanned by Tescan Vega-3 XMU electron microscope. The fracture was divided into three areas: fatigue crack source, fatigue expansion and fatigue transient, as shown in Fig. 10. The fatigue crack initiation zone was generally located on the specimen surface where stress is easily concentrated. The fatigue source of base material was generated from material defects, accompanied with river pattern radiation toward the inside of specimens ; Fatigue strip was the main feature of the crack propagation zone, and secondary cracks were evident. The fracture of base materials appeared like stepped spindrifts during the crack propagation stage.

Table 8
Comparison of fatigue strength values.

Specimen type	95% survival probability (MPa)					
	$N = 5 \times 10^5$		$N = 1 \times 10^6$		$N = 2 \times 10^6$	
	net section	gross section	net section	gross section	net section	gross section
Q460 base material	308.98	–	294.45	–	280.60	–
Q690 base material	413.39	–	394.05	–	375.63	–
Q460 perforated plate	203.61	150.83	183.32	135.80	165.06	122.27
Q690 perforated plate	240.56	178.21	219.60	162.68	200.47	148.51
Q460 bolted connection (pretension force 170 kN)	318.31	212.25	255.52	170.38	205.12	136.77
Q690 bolted connection (pretension force 170 kN)	442.34	294.89	369.68	246.45	308.95	205.96

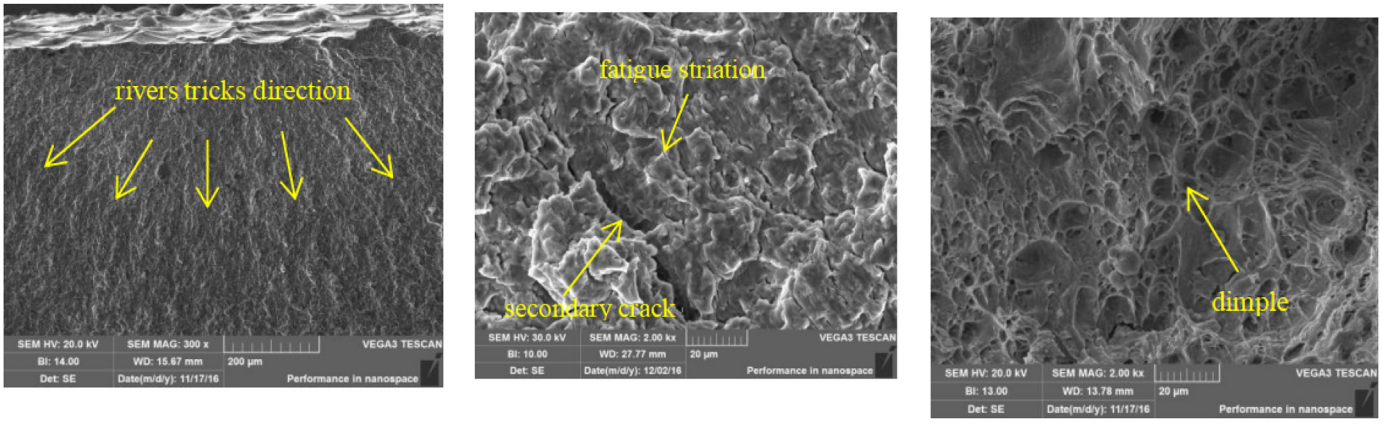

(a) Crack initiation region (b) Crack propagation region (c) Instant fracture region

Fig. 10. Fracture morphology of base material.

Secondary cracks were mainly distributed in step profiles. Fatigue strips on the fracture were approximately parallel. The fracture strips extended toward the same direction of secondary cracks and perpendicular to the crack propagation direction ; The presence of dimples was the main feature of the transient fracture zone, and a large dimple can be observed in the transient region of the base material.

4.4. Fatigue damage

The fatigue life of structures involves microcrack initiation, propagation, and fracture processes. Crack propagation is a process of cumulative damage. The damage accumulates to a certain extent, and then the structure fractures. The degree of damage is measured by damage quantity D [32,33], which serves as reference for Eqs. (13) and (14). In this study, the high-cycle fatigue damage model [34] is used to calculate D. The formulas are as follows:

$$N_f = \frac{(\beta + 1)(S_{\max}^{\beta+1} - S_{\min}^{\beta+1})^{-1}}{2B(\beta + 2)}, \tag{13}$$

$$D = 1 - \left(1 - \frac{N}{N_f}\right)^{1/(\beta+2)}, \tag{14}$$

where B and β are the material constants determined from the test; S_{max} and S_{min} are the maximum and minimum stresses, respectively; and N_f, N ,and D are the fatigue life, number of fatigue cycles, and cumulative fatigue damage, respectively.

β could be gained from the regression of the test data (Table 9).

The fatigue damage curve (Fig. 11) could be drawn according to Eq. (14) after the values of β were obtained.

As shown in Fig. 11, the damage development laws of Q469 and Q690 steel fatigue specimens were consistent. As the number of fatigue increases, the D value increases slowly, the slope of the curve increases, and the damage develops faster and faster. Under the same damage fraction, the damage development rate of the bolted connection was the fastest, followed by that of the perforated plate. The damage development rate of the base material was the slowest. As the ratio of N to N_f approached 1, D increased transiently. This finding showed that the effective bearing area of the specimens decreased because of material damage. The residual section was inadequate for resisting stress caused by external loads; hence, the specimens developed transient fracture. The transient fracture stage accounted for a relatively small proportion of fatigue life, which indicated that this stage was not fully developed.

Table 9
The value of β.

Specimen type	Base metal	Perforated plate	Bolted connection
Q460D	13.3864	5.6050	2.1546
Q690D	13.4718	6.6046	2.8625

5. Conclusions

This study discussed the fatigue performances of high strength steel Q460 and Q690 and bolted connections. A fatigue test was performed for the base materials, perforated plates, and bolted connections. The following conclusions could be drawn.

(1) The base materials of Q460 and Q690 showed good fatigue performance in the finite fatigue range. The fatigue strength was significantly higher than the code value. The fatigue strength under the 95% survival probability of the Q690 base material was 1.3 times that of the Q460, and the fatigue strength increased with the steel strength.
(2) Under the 95% survival probability, the fatigue strengths of the Q690 perforated plate were 2.3, 2.1, and 2.2 times the code values of AISC360, BS7608, and Eurocode3, respectively. For the Q460 perforated plate, its fatigue strengths were 1.9, 1.7, and 1.8 times those of AISC360, BS7608, and Eurocode3. The perforated plates showed good performance in the finite fatigue range, and the specifications were relatively conservative. The Q690 fatigue strength under the 95% survival probability was 1.2 times that of Q460. The fatigue strength of the perforated plates increased with the strength of the steel.
(3) The AISC360 and BS7608 design curves were applicable for the fatigue life analysis of the Q460 bolted connection and showed it possessed adequate safety margins. The EC3 curve was relatively conservative. The fatigue performance of the Q690 bolted connection was significantly superior to the Q460. The fatigue strength under the 95% survival probability of Q690 was 1.5 times that of Q460.
(4) The stress concentration increased the local stress and restricted the crack initiation position. The influence on fatigue strength was remarkable.
(5) The bolt pretension force weakened the degree of stress concentration around the hole and prevented the fatigue crack from initiating at the net section. The fatigue crack transferred to the area in front of the hole. in the finite fatigue range, the fatigue performance of the bolted connection at the net section was calculated to be similar to that of the base material.
(6) The discreteness of the test data on the bolted connection was large. Many other factors may affect the fatigue strength of the bolt

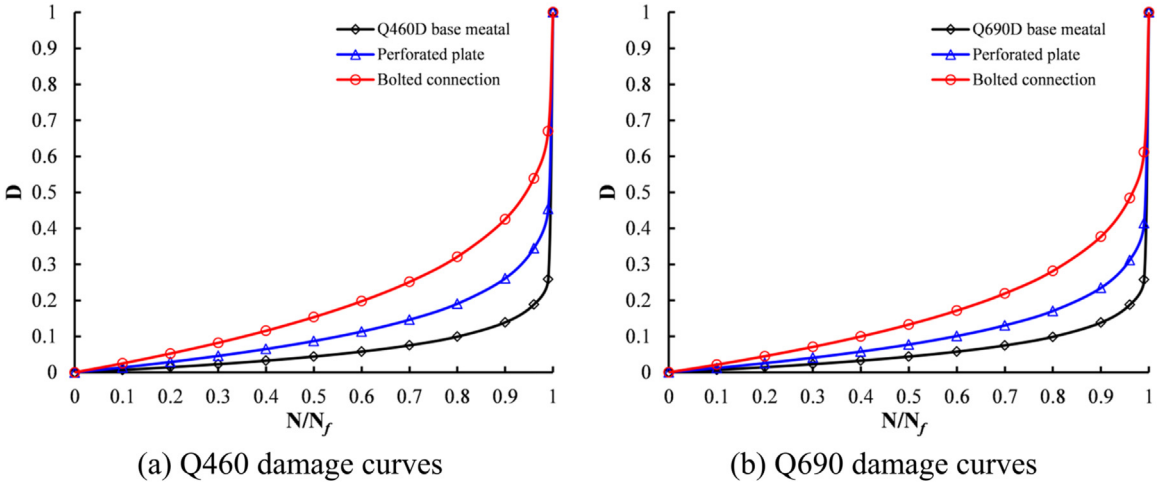

Fig. 11. Fatigue damage curves.

besides the steel strength and stress concentration. It is also affected by the loading stress amplitude, bolted layout, bolt pretension force, bolted diameter, diameter of the bolted hole, and surface treatment. Additional experimental data are needed for the comprehensive evaluation of the fatigue performances of bolted connections of high-strength steel.

Acknowledgment

The authors would like to thank the National Natural Science Foundation of China (No. 51308454) and the State Key Laboratory Base of Eco-hydraulic Engineering in Arid Area (No. 2017ZZKT-8) for their financial support.

References

[1] X.M. Cao, G.Y. Yu, Influence factors and design of bolt joint fatigue strength, J. Ind. Constr. 16 (8) (1986) 14–21 (in Chinese).
[2] H. Sehitoglu, Fatigue life prediction of notched members based on local strain and elastic–plastic fracture mechanics concepts, J. Eng. Fract. Mech. 18 (3) (1983) 609–621.
[3] G. Josi, G.Y. Grondin, G.L. Kulak, Fatigue of bolted connections with staggered holes, J. J. Bridge Eng. 9 (6) (2004) 614–622.
[4] N.E. Dowling, Mechanical Behavior of Materials: Engineering Methods for Deformation, Fracture, and Fatigue, M. Prentice Hall., 1999, pp. 649–705.
[5] J.M. Alegre, A. Aragon, F.A. Gutierrez-Solana, Finite element simulation methodology of the fatigue behavior of punched and drilled plate components, J. Eng. Fail. Anal. 11 (2004) 737–750.
[6] L. Sanchez, F. Gutierrez-Solana, D. Pesquera, Fatigue behavior of punched structural plates, J. Eng. Fail. Anal. 11 (5) (2004) 751–764.
[7] J.M. Minguez, J. Vogwell, Effect of torque tightening on the fatigue strength of bolted joints, J. Eng. Fail Anal. 13 (2006) 1410–1421.
[8] A. Benhamena, A. Amrouche, A. Talha, N. Benseddiq, Effect of contact forces on fretting fatigue behavior of bolted plates: numerical and experimental analysis, J. Tribol. Int. 48 (2012) 237–245.
[9] A. Benhamena, A. Talha, N. Benseddiq, A. Amrouche, G. Mesmacque, M. Benguediab, Effect of clamping force on fretting fatigue behavior of bolted assemblies: case of couple steel–aluminium, J. Mater. Sci. Eng. A 527 (2010) 6413–6421.
[10] M. Saranik, L. Jézéquel, D. Lenoir, Experimental and numerical study for fatigue life prediction of bolted connection, Proc. Eng. J. 66 (2013) 354–368.
[11] Z.Y. Wang, L.H. Li, Y.J. Liu, Q.Y. Wang, Fatigue property of open-hole steel plates influenced by bolted clamp-up and hole fabrication methods, J. Mater. 9 (8) (2016) 1–10.
[12] Z.Y. Wang, N. Zhang, Q.Y. Wang, Tensile behavior of open-hole and bolted steel plates reinforced by CFRP strips, J. Compos. Part B: Eng. 100 (2013) 101–113.
[13] Janne Juoksukangas, Arto Lehtovaara, Antti Mäntylä, Experimental and numerical investigation of fretting fatigue behavior in bolted joints, J. Tribol. Int. 103 (2016) 440–448.
[14] H.T. Chen, Gilbert Y. Grondin, Robert G. Driver, Characterization of fatigue properties of ASTM A709 high performance steel, J. J. Constr. Steel Res. 63 (6) (2007) 838–848.
[15] D.P. Davies, Duplex hardening: an advanced surface treatment, J. Heat Treat. 2 (1992) 38–46.
[16] N. Jezernik, S. Glodez, T. Vuherer, B. Spes, J. Kramberger, The influence of plasma cutting process on the fatigue strength of high strength steel S960Q, J. Key Eng. Mater. 0 (348) (2007) 669–672.
[17] S. Cicero, T. García, J.A. Álvarez, A. Klimpel, A. Bannister, A. Martín-Meizoso, Fatigue behavior and BS7608 fatigue classes of steels with thermally cut holes, J. J. Constr. Steel Res. 128 (2017) 74–83.
[18] S. Cicero, T. García, J.A. Álvarez, A. Martín-Meizoso, A. Bannister, A. Klimpel, Definition of BS7608 fatigue classes for structural steels with thermally cut edges, J. J. Constr. Steel Res. 120 (2016) 221–231.
[19] Carlos Jiménez-Peña, Reza H. Talemi, Barbara Rossi, Dimitri Debruyne, Investigations on the fretting fatigue failure mechanism of bolted joints in high strength steel subjected to different levels of pre-tension, J. Tribol. Int. 108 (2017) 128–140.
[20] O.-P. Hämäläinen, T. Björk, Fretting fatigue phenomenon in bolted high-strength steel plate connections, Steel Constr. 8 (2015) 174–178.
[21] EN 1993-1-8, Eurocode 3: Design of Steel Structures-Part 1-8: Design of Joints, European Committee for Standardisation, Brussels, 2005.
[22] DASt-Richtlinie/Deutscher Ausschuß für Stahlbau, Band 103: Nationales Anwendungsdokument (NAD), Richtlinie zur Anwendung von DIN V ENV, Eurocode 3, 1993.
[23] EN 1993-1-12, Eurocode 3: Design of Steel Structures-Part 1–12: Additional Rules for the Extension of EN 1993 up to Steel Grades S 700, European Committee for Standardisation, Brussels, 2007.
[24] EN 1993-1-8, Eurocode 3: Design of Steel Structures-Part 1-8: Fatigue, European Committee for Standardisation, Brussels, 2005.
[25] BS7608:2014, Guide to Fatigue Design and Assessment of Steel Product, British Standards Institution, London, UK, 2014.
[26] European Committee for Standardization (CEN), EN 1993-1-9 Eurocode3, Design of Steel Structures - Part 1–9: Fatigue, CEN, Brussels, 2005.
[27] ANSI/AISC360-10 Specification for Structural Steel Buildings. S. American Institute of Steel Construction, June 22, 2010.
[28] GB/T 2975-2018, Steel and Steel Products-location and Preparation of Test Pieces for Mechanical Testing, China Standard Press, BeiJing, 2018.
[29] GB50017-2018, Code for Sesign of Steel Structures, China Plainning Press, BeiJing, 2017.
[30] GB/T228.1-2010, Metallic Materials-Tensile testing-Part 1: Method of Test at Room Temperature, Standard Press of China, BeiJing, 2012.
[31] H.G. Lei, Y. Pei, L.J. Liu, FEA analysis of fatigue notch coefficients for high strength bolts, J. Eng. Mech. 25 (2008) 49–53.
[32] H.G. Lei, J.P. Bai, The test research of suspended crane's dynamic influence to fatigue loading spectrum of grid structure, Steel Struct. (2006) (in Chinese).
[33] H.G. Lei, J. Zhang, The calculation method of the fatigue reliability index of high strength bolt in the grid structure with bolt-sphere joints, Steel Struct. (2006) (in Chinese).
[34] Z.X. Li, T.H.T. Chan, J.M. Ko, Fatigue damage model for bridge under traffic loading: application made to Tsing Ma Bridge, J. Theor. Appl. Fract. Mech. 35 (2001) 81–91.